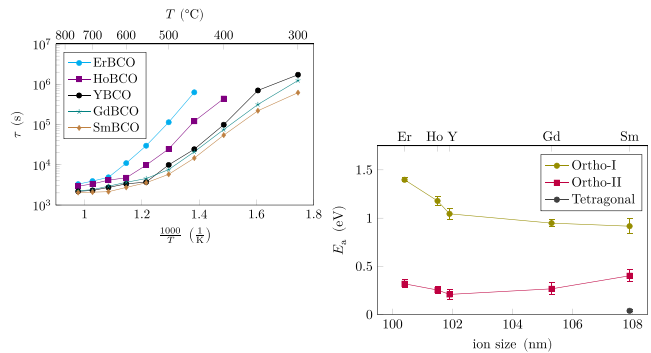


# Determination of the Oxygen Chain Ordering in REBa<sub>2</sub>Cu<sub>3</sub>O<sub>7-δ</sub> by Electrical Conductivity Relaxation Measurements

Pablo Cayado,\* Daniel Hauck, Dominic Barthlott, Manuela Erbe, Jens Hänisch,\* and Bernhard Holzapfel

**ABSTRACT:** Electrical conductivity relaxation was measured to investigate the kinetics of oxygen incorporation (in-diffusion process) and excorporation (out-diffusion process) in different epitaxial REBa<sub>2</sub>Cu<sub>3</sub>O<sub>7-δ</sub> thin films prepared by chemical solution deposition. The oxygen diffusion in these compounds happens in two distinct regimes with different activation energies, which depend on the compound. As the detailed X-ray analysis of similarly processed REBa<sub>2</sub>Cu<sub>3</sub>O<sub>7-δ</sub> films revealed, the transition temperature between these two regimes is compatible with a transition in the oxygen ordering in the Cu–O chains from the Ortho-II phase to the Ortho-I phase. These transitions may be of great importance for further optimization of the oxygenation process during the synthesis of these compounds but may depend not only on the rare-earth (RE) element but also on further factors such as variations of stoichiometry. The presented electrical conductivity measurements provide easy access to the determination of these transition temperatures.

**KEYWORDS:** electrical conductivity, oxygen ordering, ortho phase, REBCO, activation energy



## INTRODUCTION

Functional oxides are a vast group of compounds, which gained great interest in many different fields. For decades, new physical properties of these compounds have been discovered that have revealed their enormous potential for novel applications: optoelectronic devices, photocatalysts, information and energy storage, water splitting, ferroelectrics, ferromagnets, superconductors, and so forth. These exceptional physical properties are strongly related to their electronic structures, surface morphology, interfaces, microstructure, defect landscape, and strain state, among others. Therefore, the study of the effects of these factors on the different functionalities is a key step in achieving practical applications of these oxides. Among the multiple functional oxides, superconductors and, in particular, high-temperature superconductors are among the most studied in the last two decades. Their ability to save energy by reducing the electrical resistance to zero at temperatures even above 77 K makes them extremely attractive for use in the form of wires in many different applications such as generators, motors, or in the electrical grid. The spread of their use would mean a step toward a very efficient and therefore environmentally friendly power technology. In recent years, REBa<sub>2</sub>Cu<sub>3</sub>O<sub>7-δ</sub> (REBCO, RE—rare earth) compounds have attracted the attention of both research and industry since their properties, especially

their high critical temperature ( $T_c$ ) and large current-carrying capability even at high fields, promise applicability in multiple power and high-field devices if fabricated as coated conductors (CCs).<sup>1–4</sup> The crystallographic structure of the REBCO compounds depends on the value of  $\delta$  (i.e., the oxygen content): it is tetragonal for high values of  $\delta$  and orthorhombic for low  $\delta$  values, where  $\delta$  itself depends on temperature and oxygen partial pressure in thermodynamic equilibrium, and only the orthorhombic phase(s) shows superconductivity at a finite critical temperature  $T_c$ . Therefore, the tetragonal/orthorhombic transition depends on the particular conditions under which the oxygen is introduced in the structure. For example, in YBCO, the phase transition takes place at  $\sim 700$  °C in a pure oxygen atmosphere for  $\delta \sim 0.5$ .<sup>5–8</sup> In the orthorhombic structure, the oxygen atoms start to incorporate periodically in the Cu–O chains, forming superstructures (different arrangements of oxygen atoms in the Cu–O chains, which extend into multiple unit cells), which have different

periodicities along the  $a$ -axis.<sup>6</sup> Kinetic effects may preclude the formation of such types of oxygen-ordered structures. Nevertheless, De Fontaine et al. proposed an equilibrium phase diagram of the different superstructures depending on the oxygen content and temperature.<sup>5</sup> Understanding the mechanism behind these changes in the oxygen content and ordering is a key point in controlling the final superconducting properties of the CCs. Besides, it will also allow a better comprehension of other phenomena related with the oxygen content in REBCO films as, for example, the resistive switching.<sup>9,10</sup>

Within the family of REBCO,  $\text{YBa}_2\text{Cu}_3\text{O}_{7-\delta}$  (YBCO) is probably the best-known and -studied compound since it was the first superconductor showing a  $T_c$  above liquid-nitrogen temperature (LN<sub>2</sub>, 77 K). However, there are other REBCO compounds that could exhibit better electrical properties than YBCO aside from small improvements in  $T_c$  and, therefore, be very attractive materials to be studied in depth.<sup>11–15</sup> These improved properties originate from variations in the electronic structure, the valence states, and, ultimately, the ionic radii of the RE<sup>+3</sup> ions within the structure.<sup>16–19</sup> On the other hand, in order to spread the use of high- $T_c$  superconductors, it is necessary to develop low-cost techniques for the fabrication of high-performance REBCO CCs such as chemical solution deposition (CSD). CSD, which was employed to prepare the samples in this work (in particular, following the well-known TFA-MOD route<sup>20</sup>), is a very competitive, cost-effective, and scalable method to produce REBCO epitaxial films; therefore, an extensive analysis of all the relevant processing steps is worthwhile.<sup>21–24</sup> A very important step in any CC manufacturing process is oxygenation. Achieving the optimal oxygen content in REBCO films is a critical issue in the development of high-critical current superconductors. This oxygenation process requires an exhaustive knowledge about how oxygen diffuses into the films. The diffusion process has been studied previously in multiple studies,<sup>25–32</sup> and in most of the cases, the kinetics of oxygen exchange have been analyzed in terms of a volume diffusion process governed by Fick's laws. However, in recent years, this process has been treated in a different perspective, giving more importance to the surface reactions, which may be the slowest step in the whole chain of oxygen exchange. Following this perspective, Cayado et al. have explained oxygen diffusion in the case of YBCO films as a surface-controlled process with several surface reactions linked together, in which the chemisorption process leading to the formation of ionized molecules or the dissociation of the molecules leading to the formation of ions at the surface is the rate-determining step (rds) for these films.<sup>33</sup> However, possible differences in the oxygen diffusion in REBCO films with different RE ions have not been deeply studied yet. For this reason, we studied the oxygen diffusion process on several REBCO films in detail with the aim of explaining the kinetics of the diffusion process and the structural changes that occur during oxygenation in each compound.

## THEORETICAL BACKGROUND

The problem of oxygen diffusion in REBCO films of (sufficiently small) thickness  $l$  can be treated, in a simple way, as a one-dimensional diffusion process in a homogeneous medium enclosed by two parallel infinite planes at positions  $x = 0$  and  $x = l$ . These conditions are the same as considering a plane lamella of a material so thin that all the diffusing matter

enters the material through the plane faces and a negligible amount through the edges. In this case, the problem is reduced to solving Fick's second law in one dimension<sup>34</sup>

$$\frac{\partial C(x)}{\partial t} = D\Delta C \quad (1)$$

with  $C$  as the molar concentration,  $t$  the time in which the diffusion is taking place, and  $D$  the material-dependent diffusion coefficient. Two boundary conditions can then be established: (1) there is no flow through the substrate ( $x = 0$ )<sup>33</sup>

$$J(0) = -D\frac{\partial C(x)}{\partial x}\Big|_{x=0} = 0 \Rightarrow \frac{\partial C(x)}{\partial x}\Big|_{x=0} = 0 \quad (2)$$

and (2) in first approximation, it can be assumed that at the surface ( $x = l$ ), the concentration gradient depends linearly on the difference between equilibrium concentration  $C_{\text{eq}}$  and surface concentration  $C_S$ <sup>35</sup>

$$\frac{\partial C(x)}{\partial x}\Big|_{x=l} = k(C_{\text{eq}} - C_S) \quad (3)$$

where  $k$  is the surface reaction rate,  $C_{\text{eq}}$  is the concentration when the equilibrium is reached, and  $C_S$  is the current concentration at the surface. Solving the differential equations for these boundary conditions, the following expression is obtained<sup>33,35</sup>

$$\frac{\bar{C}(t) - C_0}{C_{\text{eq}} - C_0} = 1 - \sum_{n=1}^{\infty} \frac{2\gamma^2}{\beta_n^2(\beta_n^2 + \gamma^2 + \gamma)} \quad (4)$$

where  $\gamma = lk/D$  is a sample constant,  $\tau$  is the relaxation time for the surface-controlled process, and  $\beta_n$  represents the  $n$ th positive root of

$$\gamma = \beta \tan(\beta) \quad (5)$$

Considering that the largest contribution of the sum in eq 4 is given by the first term and the others are negligible and that the conductance,  $G$ , is proportional to the average oxygen concentration,<sup>33</sup> eq 4 can be simplified as

$$\frac{G(t) - G_0}{G_{\infty} - G_0} = 1 - Ae^{-t/\tau} \quad (6)$$

with some constant  $A$ , which depends on  $\gamma$ . The temperature dependence of the relaxation time,  $\tau$ , can be written as<sup>28</sup>

$$\tau(T) = \tau_0 e^{E_0/k_B T} \quad (7)$$

$$\ln(\tau(T)) = \ln(\tau_0) + \frac{E_a}{k_B T} \quad (8)$$

The activation energy ( $E_a$ ) of the process can, therefore, be obtained by a linear fit of a natural logarithmic plot of  $\tau$  over  $1/T$ ; see Figure 1. Note that for bulk-dominated diffusion processes, the expression would have the same form, but  $\tau$  would be determined by the bulk processes instead. An example can be found in ref 29.

## TRANSITION TEMPERATURE TO THE ORTHO-I PHASE

Figure 1a displays the temperature dependence of  $\tau$  for the out-diffusion process for REBCO films with RE = Er, Ho, Y, Gd, and Sm. As expected, the  $\tau$  values are larger at lower temperatures in all films. The most interesting feature is a clear

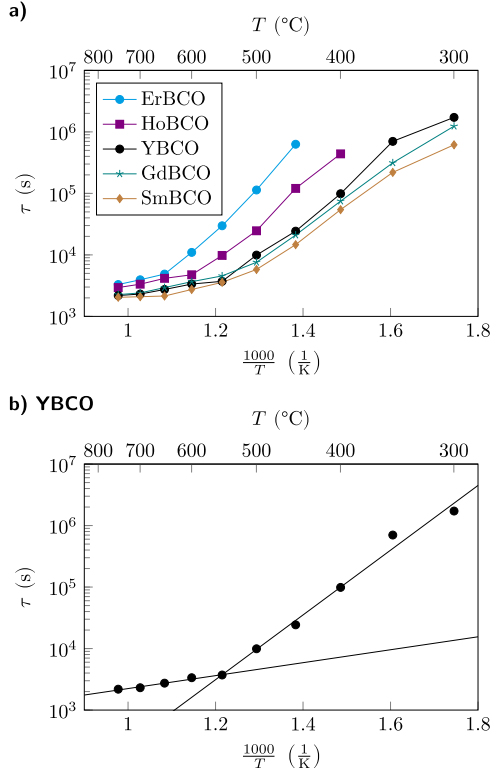


**Figure 1.** (a) Dependence of the relaxation time on temperature for the out-diffusion process of several REBCO films. (b) Example for the determination of the activation energies and the transition temperature (intersection point of the two lines).

change in the slope at a specific temperature for every RE element, that is, in the activation energy  $E_a$  (eq 8). Figure 1b shows the two determined slopes using YBCO as an example. The transition temperature is given by the intersection point of the straight lines. The same change in  $E_a$  was shown by Cayado et al. for the out-diffusion process of YBCO films when varying the temperature,<sup>33</sup> and a similar effect was reported by Krauns et al. on YBCO films when the oxygen partial pressure was varied.<sup>30</sup> This latter publication reported a kink in  $\ln(R)$  versus  $\ln(p_{O_2})$  and explained it by assuming that the electrical resistance of the films depends on the oxygen content and the structure of the compound. Accordingly, the tetragonal-orthorhombic (T-O) transition should be indicated by a sharp change in the electrical behavior of the films. Considering these results, it sounds plausible that the observed change in  $E_a$ , shown in Figure 1, may be attributed to the T-O transition.

Furthermore, if the temperatures of this transition (kink temperatures) are plotted against the  $RE^{3+}$  ion size (Figure 2), a systematic decrease in the transition temperature with increasing ion size, that is, a very similar trend to the one reported by Su et al.<sup>36</sup> for a transition temperature in bulk samples, is observed. Remarkably, however, the transition temperatures of Su et al. are overall around 100  $^{\circ}C$  higher.

In order to possibly relate the observed transition with the T-O transition, a detailed analysis of the  $T_c$  values of the films was carried out. If it is indeed the T-O transition, a change in  $T_c$  from zero to finite values should be observed since the tetragonal phase is not superconducting. However, in general, this is not observed when plotting  $T_c$  versus  $c$ -axis and  $T_{oxy}$  (Figure 3). Only for SmBCO films,  $T_c = 0$  is observed for  $T_{oxy}$

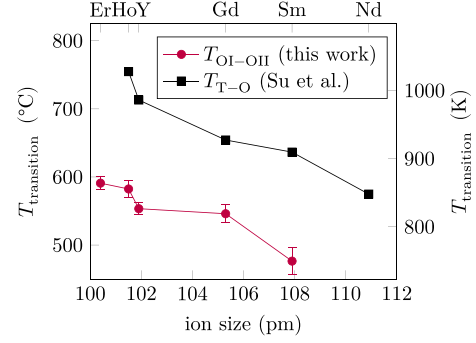


**Figure 2.** RE ion size dependence of the transition temperatures (second transition in the case of SmBCO) between the regimes with different  $E_a$ , determined from the electrical conductance measurements (blue) compared with the T-O transition temperatures by Su et al.<sup>36</sup>

> 600  $^{\circ}C$ , meaning that the T-O transition happens around this temperature for an oxygen partial pressure of 1 atm. In fact, the SmBCO curve in Figure 1 presents two kinks. The first one happens around 650  $^{\circ}C$ , and this value is very similar to the one reported by Su et al. for SmBCO bulk samples,<sup>36</sup> as shown in Figure 2. However, the second kink temperature of around 450  $^{\circ}C$  lies significantly lower. Therefore, apart from this first kink for SmBCO, the kink transition should have a different origin than the T-O transition. At  $T_{oxy} < 250$   $^{\circ}C$ , zero  $T_c$  values are obtained for all films (not shown in Figure 3) because at such low temperatures, diffusion processes are not taking place in reasonable timescales.

At first glance, the curves in Figure 3 appear very similar in shape. However, if they are observed carefully, there are remarkable differences. Focusing on YBCO, it is possible to distinguish three different regions. The first one is a plateau at low  $T_{oxy}$ . In this region,  $T_c$  is quite stable and reaches its largest value around 92 K. In the following second region, for 400  $^{\circ}C < T_{oxy} < 500$   $^{\circ}C$ , the  $T_c$  values decrease, and finally, for  $T_{oxy} > 500$   $^{\circ}C$ , the  $T_c$  values tend to stabilize again but this time at values around 60 K. This third region is commonly known as the “quasi plateau” and was reported several times in the past for different REBCO compounds.<sup>37–39</sup> The dependence of  $T_c$  on the  $c$ -axis parameter follows the same trend. In the first region, for low values of the  $c$ -axis,  $T_c$  values are stable around 92 K. Then, at a certain  $c$ -axis value,  $T_c$  starts to decrease until it becomes stable again at around 60 K for larger  $c$ -axis values. This particular shape of the  $c$ -axis versus  $T_c$  curve with the presence of several (quasi) plateaus is not completely understood yet. However, the most accepted explanation is that every particular way in which the oxygen is arranged in the Cu-O chains, that is, every kind of oxygen ordering, has a distinct  $T_c$ .<sup>7,40</sup> Thereby, the quasi plateau at 60 K corresponds to an Ortho-II long-range ordered superlattice, which changes to an Ortho-I phase whose characteristic  $T_c$  is  $\sim 90$  K, at a particular oxygen content that adjusts with the temperature and in turn affects the  $c$ -axis value.<sup>7,37</sup> This means that the oxygenation at higher temperatures ( $T_{oxy} > 500$   $^{\circ}C$  in this case) induces a defined order in the oxygen atoms being placed in the Cu-O chains in such a way that only some specific chains are filled giving rise to the formation of the Ortho-II phase (Cu-O chains are ideally filled following the sequence: full-empty-full-empty...) characterized by a  $T_c \sim 60$  K. The Ortho-II phase is kept in a range of oxygen content in which the oxygen atoms are able to place in the Cu-O chains

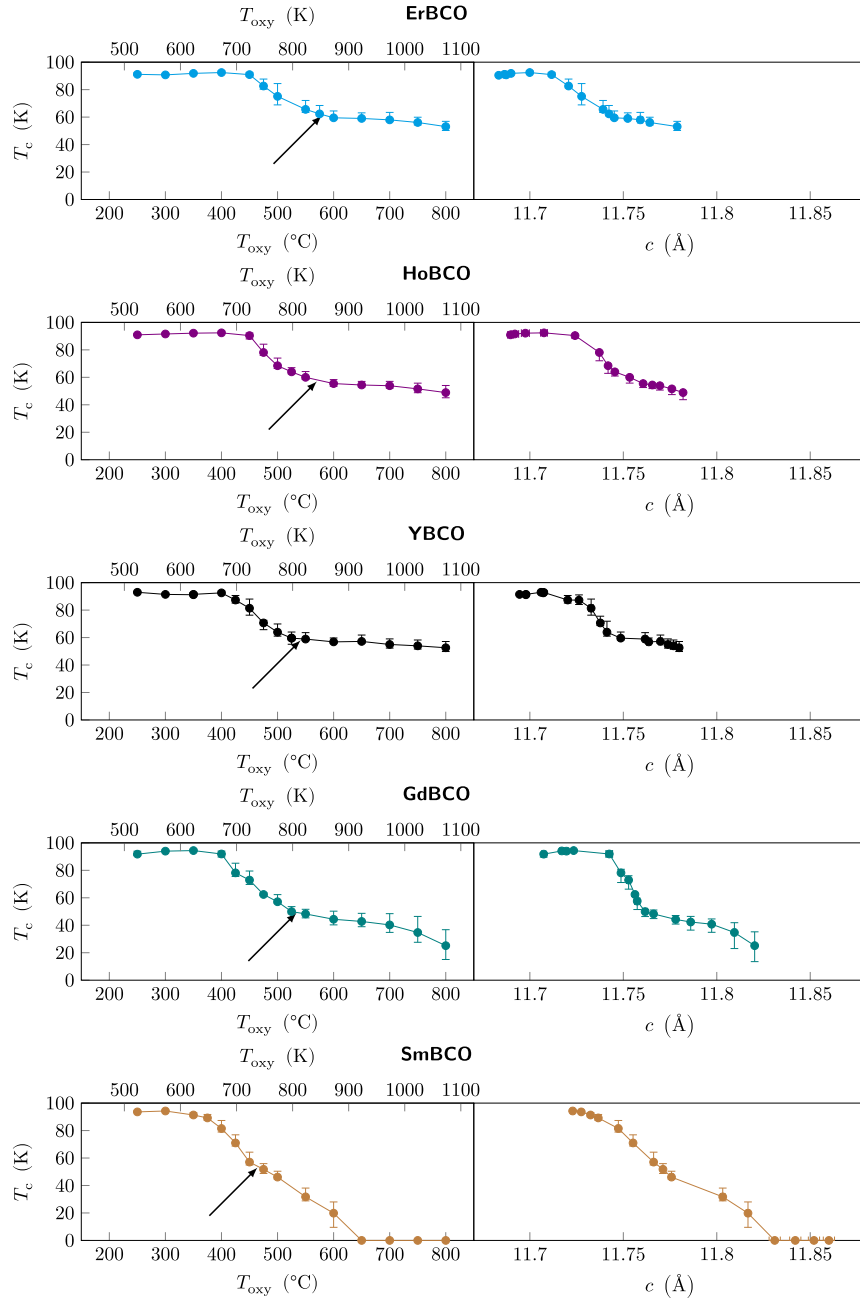


**Figure 3.**  $T_c$  values in dependence of the oxygenation temperature (left column) and  $c$ -axis length (right column) for the different REBCO compounds of this study.

according to the previously mentioned ordering but also admits certain deviations of this ideal ordering so that the phase is kept in a determined  $T_{oxy}$  range ( $\lesssim 500$   $^{\circ}$ C in this case), producing the quasi plateau at  $\sim 60$  K. At some point, as  $T_{oxy}$  is reduced more and more and, therefore, more O atoms are included in the chains occupying more places in the empty chains, the Ortho-II phase is not stable anymore, and the phase transition is reached. During this phase transition, the oxygen ordering is not well-defined causing a steeper increase in  $T_c$ . This transition state finishes at a particularly lower  $T_{oxy}$  ( $\sim 400$   $^{\circ}$ C in the case of YBCO) when a new oxygen ordering is reached and the Ortho-I phase (Cu–O chains are filled following the sequence: full–full–full–full...), in which the commonly reported  $T_c$  ( $\sim 92$  K in this case) of every compound is reached.

Considering YBCO a well-defined reference, the oxygen ordering of the other REBCO compounds can be recognized. For all of them,  $T_c$  versus  $T_{oxy}$  and  $T_c$  versus  $c$ -axis, as shown in Figure 3, show a similar first region with rather stable and high  $T_c$  values separated by a transition zone from a second region with lower  $T_c$  values, which in some cases are constant and in other cases, not. This first region with stable and high  $T_c$  values corresponds to the Ortho-I phase of every compound. At a certain RE-dependent temperature, the  $T_c$  values start to decrease. This reduction in  $T_c$  ends in a second region with, again, stable but lower  $T_c$  values ( $\sim 60$  K) in the case of ErBCO and HoBCO. This second region corresponds to the Ortho-II phase of these compounds. In contrast, this second plateau at lower  $T_c$  values is not clearly seen in the case of GdBCO and SmBCO. This fact entails that in these compounds, Ortho-II is

a short-order phase and only stable for a very specific oxygen content. Any deviation from this oxygen content causes a reordering of the oxygen which changes  $T_c$ . This is especially clear in the case of SmBCO, where the plateau associated with the Ortho-II phase is not visible at all, meaning that there is not a defined oxygen order in this region, and  $T_c$  increases with a certain slope. However, at a particular temperature, there is a sudden change in this slope indicating that the oxygen starts to place in a certain order in the Cu–O chains, initiating the transition to the Ortho-I phase, which finally leads again to the 90 K plateau at lowest oxygenation temperatures.

GdBCO is an intermediate case. At intermediate  $T_{\text{oxy}}$  ( $500^\circ\text{C} < T_{\text{oxy}} < 700^\circ\text{C}$ ), the increase in the  $T_c$  values slows down, arriving at a kind of short-order range stabilization that could be associated with the 60 K quasi plateau and, therefore, to the Ortho-II phase. For  $T_{\text{oxy}} < 500^\circ\text{C}$ , a drastic change in the slope occurs toward the transition to the 90 K plateau, that is, to the Ortho-I phase. In the following, the temperature at which the transition from the Ortho-II phase to the Ortho-I phase starts to take place will be called Ortho I–II phase (I–II) transition temperature because in GdBCO and SmBCO also, it can be assumed to be present (even though not clearly detected) just as for ErBCO, HoBCO, and YBCO though with a much shorter order range.

The I–II transition temperature for every compound (marked with arrows in Figure 3) perfectly coincides with the respective kink temperatures shown in Figure 2. This shows that the transition between these two oxygen orderings can be easily measured by electrical conductivity relaxation. This relatively simple technique is sensitive to such phase transitions and able to detect different oxygen arrangements in the Cu–O chains, which could be very important for further optimization of the oxygenation processes in REBCO films. Moreover, this measurement technique could also be used for the determination of different phase transitions or oxygen arrangements in other complex functional oxides in a fast and easy way. The trend of the Ortho I–II phase transition temperature with the  $\text{RE}^{3+}$  ion size suggests a close relationship between the temperature of the T–O transition and of the Ortho I–II phase transition. The T–O transition temperature decreases as the  $\text{RE}^{3+}$  size increases<sup>36</sup> which is the same behavior as for the Ortho I–II phase transition temperature. However, the temperature difference between the T–O transition and the Ortho I–II phase transition is not constant but decreases as well with the increasing  $\text{RE}^{3+}$  ion size. This means that the temperature range in which the different oxygen Ortho phases can coexist becomes narrower with increasing ion size, which can explain why for GdBCO and SmBCO the extension of the Ortho-II phase plateau is smaller or does not exist at all, respectively. It is important to note that to be able to predict where the Ortho-II phase is formed for every REBCO compound is of remarkable interest. This is because Ortho-II shows an electronic anisotropy intermediate between the Ortho-I YBCO phase and BSCCO phases,<sup>41</sup> and, therefore, this opens the possibility to investigate how the different  $\text{RE}^{3+}$  ions modify the intrinsic anisotropy of these compounds.

## ACTIVATION ENERGY

The activation energy,  $E_a$ , is the energy barrier that a reactant must surpass in order to undergo a certain reaction. According to Cayado et al.,<sup>33</sup> in the case of the diffusion process in YBCO films, these reactions are the surface reactions that the oxygen

molecules must complete before entering the structure of the REBCO compound. To be more precise,  $E_a$  would be the energy required to carry out the rds, which in the case of oxygen diffusion in YBCO films was found to be either the chemisorption process leading to the formation of ionized  $\text{O}_2^{2-}$  molecules or the dissociation of the molecules leading to the formation of  $\text{O}^-$  ions at the surface.<sup>33</sup> Therefore,  $E_a$  is an indirect measure of the effort the whole diffusion process needs in a certain temperature range and could be relevant information for optimizing oxygenation processes in REBCO films. However, this model was built for the diffusion process at high temperatures, that is, for the diffusion when the oxygen in the films tends to order according to the Ortho-II phase, and did not consider the change in  $E_a$  when the oxygen ordering changes to the Ortho-I phase.

According to eq 8 and Figure 1, the  $E_a$  values were defined for the two different regimes: the Ortho-II phase at higher temperatures and the Ortho-I phase at lower temperatures, as shown in Figure 4. The  $E_a$  values in the Ortho-II phase are

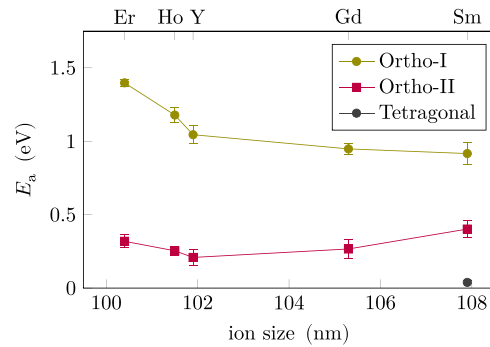


Figure 4. Dependence of the activation energy on the  $\text{RE}^{3+}$  ion size.

lower than those in the Ortho-I phase for all RE ions, and this difference is smaller for bigger ions. This means that the diffusion process, in particular the rds, is faster in the Ortho-II phase. Moreover, our  $E_a$  values for the YBCO films in the Ortho-II phase are comparable with the data reported in the past by several authors in different types of films (most of the reported data are in this range of temperature).<sup>28,32,33</sup>

The fact that the  $E_a$  values are different for distinct oxygen ordering phases in the REBCO compounds is not well understood considering that at least in the high-temperature region, one of the surface reactions is the rds. If the film surface does not suffer any alteration for decreasing  $T_{\text{oxy}}$  (to the best of our knowledge, there are no publications reporting such changes), there is no argument in this model to support a variation in  $E_a$  unless the rds itself changes. Hence, our hypothesis is that at low  $T_{\text{oxy}}$ , when the oxygen is ordered in the Ortho-I phase, the rds is not one of the surface reactions but the so-called “bulk diffusion”, that is, the diffusion within the  $a$ – $b$  planes. This is very reasonable considering the path the oxygen ions have to complete once they reach the  $a$ – $b$  planes for the different Ortho phases: in Ortho-II, only some of the Cu–O chains incorporate oxygen ions, and therefore, the filling process is relatively fast. If this process is faster than the slowest surface reaction, the diffusion would be ruled by this surface reaction. This is exactly what happens at high  $T_{\text{oxy}}$  as Cayado et al. proposed.<sup>33</sup> However, at low  $T_{\text{oxy}}$ , the Ortho-I phase is formed, and in this case, all Cu–O chains are nearly filled with oxygen. Consequently, the probability of the oxygen

ions to find a free place in their neighborhood for diffusion is much lower, and the in-plane diffusion process takes significantly longer. Now the surface reactions are likely faster than the in-plane diffusion, and the entire diffusion process is controlled by the “bulk diffusion” with diffusion within the  $a$ – $b$  planes being the new rds. This change in the rds can perfectly explain the observed change in  $E_a$ .

The dependencies of  $E_a$  on the ion size for both Ortho phases have certain similarities but are not exactly the same. In the Ortho-II phase,  $E_a$  shows a distinct minimum around the ion size of  $Y^{3+}$  and therefore follows the tendency of REBCO phase stability toward the most stable REBCO-123 phase which is YBCO. Apparently, both the RE-Ba disorder as typical for large RE ions and increased vacancies in the RE ion site as typical for small ion sizes have an impact on the oxygen diffusion activation energies and therefore decrease the overall diffusion rates. However, in the Ortho-I phase,  $E_a$  is evidently lower for bigger ions. This has already been observed in melt-textured samples and explained by the variation of the lattice constant among the different REBCO crystals and the concomitant changes in the interaction energy of O(1) and O(5) atoms.<sup>42</sup> This has important consequences for optimizing the oxygenation process of the different REBCO compounds. As  $E_a$  decreases, to carry out the oxygenation process at lower temperatures becomes possible in reasonable times. This means that for a REBCO compound with lower  $E_a$ , the overdoped state (which is reached at lower temperatures) is possible to achieve more easily. It was shown in different works<sup>43,44</sup> that the overdoped state allows to enhance the critical current density, and therefore, it is desirable to carry out oxygenation processes to reach these overdoped states. Also, for a fixed time that could be industrially reasonable, REBCO with lower  $E_a$ , that is, those with a large  $RE^{3+}$  ion size like GdBCO or SmBCO, requires lower  $T_{oxy}$  than the usual 450–500 °C for YBCO.<sup>45</sup>

## CONCLUSIONS

This work was devoted to study possible differences and similarities in the oxygen diffusion process depending on the  $RE^{3+}$  ion size in different CSD-grown REBCO films by electrical conductivity relaxation. The differences between the diffusion kinetics in the Ortho-I and Ortho-II phases (i.e., at low and high  $T_{oxy}$ , respectively), characterized by the different  $E_a$  values, are related with the different kinds of oxygen ordering in the CuO chains. This means that we have observed the transition from the Ortho-II phase to the Ortho-I phase for the first time with a sharp change in the diffusion rate dependence and therefore in the activation energies. This result shows that the electrical conductivity relaxation technique is sensitive to these changes in the oxygen ordering in functional oxides and can be used to determine similar transition temperatures in other materials. Also, the kinetics of the oxygen diffusion process depend on the particular REBCO compound and on the oxygen ordering too. A new model to explain the variation in  $E_a$  for the different Ortho phases has been proposed based on the change of the rds from the surface reactions in the Ortho-II phase to the bulk diffusion in the Ortho-I phase. The activation energies in the Ortho-I phase are lower for REBCO films with larger  $RE^{3+}$  ions. This helped to explain why REBCO compounds with a large  $RE^{3+}$  ion size require lower  $T_{oxy}$  than YBCO films and also open the possibility to achieve highly overdoped states in these compounds in a reduced time per oxygenation process.

## METHODS

**Sample Preparation.** The preparation method for the different REBCO-TFA solutions has been described in ref 15. In summary, the precursor salts of RE, Ba, and Cu (acetates; purity >99.99%, Alfa Aesar) are mixed in the stoichiometric ratio 1:2:3 in deionized water and trifluoroacetic acid (99.5+%, Alfa Aesar). Then, the mixture is dried using a rotary evaporator, and the remaining solid residue is re-dissolved in anhydrous methanol (99.9%). The final volume of methanol is adjusted to obtain a concentration of 0.25 mol/l. The 220 nm-thick REBCO films are prepared by first depositing the precursor solutions on  $10 \times 10 \text{ mm}^2$  (100)-oriented  $LaAlO_3$  single-crystal substrates via spin coating (6000 rpm for 30 s). Before deposition, gold wires are attached with silver paste in the four corners of the substrate to provide the electrical connections with the measurement equipment later on (Figure 5). The subsequent “standard” pyrolysis and growth processes are described in ref 46.



**Figure 5.** Conductance measurement system with a REBCO sample mounted and contacted.

**Electrical Conductivity Relaxation Measurements.** The films' conductance was determined in a 5 cm wide tubular furnace by electrical measurements with a homemade 4-probe system in the Van der Pauw configuration similar to experiments reported elsewhere.<sup>31,47–50</sup> The samples were mounted on an alumina plate and contacted by CuNi44 wires that were led out of the furnace using alumina tubes (Figure 5). These wires were connected to an HP 34410A multimeter, which recorded the conductance values.

The measurements were carried out at ambient pressure in two different atmospheres: pure  $O_2$  to induce the in-diffusion process (incorporation of O atoms in the structure) and pure Ar to induce the out-diffusion process (outflow of O atoms from the structure). The measurement protocol consisted of heating the samples to 750 °C under pure Ar and then changing the atmosphere to pure  $O_2$  and keeping it for 15 min. After that, the gas was changed back to Ar and held for 1 h. Then, the temperature was decreased by 50 °C, and the procedure was repeated (Figure 6 a). At lower temperatures (<500 °C), the diffusion processes became rather slow, so the  $O_2$  atmosphere was kept longer in order to measure a reasonable change in conductance. The measurements were continued down to 300 °C. The conductance steps corresponding to oxygen out-diffusion were well fitted using eq 6, and the  $\tau$  values were thus obtained (Figure 6b). The fittings of the in-diffusion transients with eq 6 were equally good, but the fact that the  $\tau$  values were much smaller than those of the out diffusion increased the uncertainty of the measurements and the later analysis of the results.

**Quench Processes.** In order to correlate the conductance with possible structural changes of the films, a detailed X-ray diffraction (XRD) study of the REBCO films was carried out. Before the XRD measurements, these films were subjected to the same thermal processes as the films used in the conductance measurements. The films were heated up to the objective temperature under an Ar atmosphere. At this temperature, the gas was changed to  $O_2$  and kept for the same time as in the conductance measurements. After that, the films were quenched by immediately moving them from the hot zone of the furnace, and the gas was changed back to Ar. This quench procedure allows very fast cooling rates (>200 °C/min in the first 300 °C of decay) and, therefore, for freezing the oxygen content at the equilibrium value of the respective oxygenation temperature  $T_{oxy}$  by avoiding oxygen in- or out-diffusion during cooldown. The gas during the cooldown was Ar, which, as mentioned before, induces the out-diffusion process. Nevertheless, as can be seen in Figure 6a, the out-

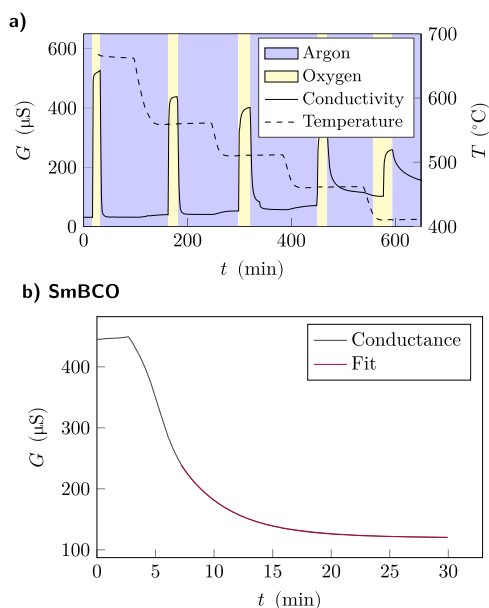


**Figure 6.** Example of the measurement protocol: (a) conductance measurements carried out at different temperatures and (b) example fit on an out-diffusion conductance measurement for obtaining the  $\tau$  value.

diffusion is much slower than the in-diffusion. Therefore, considering the high cooling rates and the slow nature of the out-diffusion process, the oxygen content of the quenched films is presumed to correspond to the temperature at which the quench started. Depending on  $T_{\text{oxy}}$ , we estimate 5% of maximum variation of the oxygen content with respect to the initial value.

**Thin-Film Characterization.** The  $c$ -axis of the quenched films was determined by XRD using a Bruker D8 diffractometer with  $\text{Cu K}\alpha$  radiation in Bragg–Brentano geometry via the Nelson–Riley procedure.<sup>51,52</sup> The  $T_c$  values ( $T_{c,90}$ ,  $T_{c,50}$ , and  $T_{c,10}$ , i.e., the temperature at which the resistance is 90, 50, or 10% of the normal-state value just above  $T_c$ , respectively) and  $\Delta T_c$  ( $T_{c,90} - T_{c,10}$ ) were studied with a 14-T quantum design physical property measurement system.

## AUTHOR INFORMATION

### Corresponding Authors

**Pablo Cayado** – Department of Quantum Matter Physics (DQMP), University of Geneva, 1211 Geneva, Switzerland; Institute for Technical Physics, Karlsruhe Institute of Technology, 76344 Eggenstein-Leopoldshafen, Germany; [orcid.org/0000-0003-3703-6122](https://orcid.org/0000-0003-3703-6122); Email: [pablo.cayado@unige.ch](mailto:pablo.cayado@unige.ch)

**Jens Hänisch** – Institute for Technical Physics, Karlsruhe Institute of Technology, 76344 Eggenstein-Leopoldshafen, Germany; Email: [jens.haenisch@kit.edu](mailto:jens.haenisch@kit.edu)

### Authors

**Daniel Hauck** – Institute for Theoretical Solid State Physics, Karlsruhe Institute of Technology, 76131 Karlsruhe, Germany; Institute for Technical Physics, Karlsruhe Institute of Technology, 76344 Eggenstein-Leopoldshafen, Germany

**Dominic Barthlott** – Institute for Technical Physics, Karlsruhe Institute of Technology, 76344 Eggenstein-Leopoldshafen, Germany

**Manuela Erbe** – Institute for Technical Physics, Karlsruhe Institute of Technology, 76344 Eggenstein-Leopoldshafen, Germany

**Bernhard Holzapfel** – Institute for Technical Physics, Karlsruhe Institute of Technology, 76344 Eggenstein-Leopoldshafen, Germany

### Author Contributions

P.C. and D.H. carried out the preparation and characterization of the films and the data analysis and wrote the paper. D.B. contributed to film characterization and data analysis. M.E. and J.H. were involved in the interpretation of the data. B.H. supervised the work. All authors discussed the results and contributed to the paper.

### Notes

The authors declare no competing financial interest.

Source data for the main paper figures are provided with this paper. Additional data are available from the corresponding authors upon request.

## REFERENCES

- (1) Iijima, Y.; Tanabe, N.; Ikeno, Y.; Kohno, O. Biaxially Aligned  $\text{YBa}_2\text{Cu}_3\text{O}_{7-x}$  Thin Film Tapes. *Phys. C* **1991**, 185–189, 1959–1960.
- (2) Hasegawa, K.; Fujino, K.; Mukai, H.; Konishi, M.; Hayashi, K.; Sato, K.; Honjo, S.; Sato, Y.; Ishii, H.; Iwata, Y. Biaxially Aligned YBCO Film Tapes Fabricated by All Pulsed Laser Deposition. *Appl. Supercond.* **1996**, 4, 487–493.
- (3) Goyal, A.; Paranthaman, M. P.; Schoop, U. The RABiTS Approach: Using Rolling-Assisted Biaxially Textured Substrates for High-Performance YBCO Superconductors. *MRS Bull.* **2004**, 29, 552–561.
- (4) Lee, J.-H.; Lee, H.; Lee, J.-W.; Choi, S.-M.; Yoo, S.-I.; Moon, S.-H. RCE-DR, a Novel Process for Coated Conductor Fabrication with High Performance. *Supercond. Sci. Technol.* **2014**, 27, 044018.
- (5) de Fontaine, D.; Ozolins, V.; Islam, Z.; Moss, S. C. Origin of Modulated Structures in  $\text{YBa}_2\text{Cu}_3\text{O}_{6.63}$ : A First-Principles Approach. *Phys. Rev. B: Condens. Matter Mater. Phys.* **2005**, 71, 212504.
- (6) Andersen, N. H.; von Zimmermann, M.; Frello, T.; Käll, M.; Mønster, D.; Lindgård, P.-A.; Madsen, J.; Niemöller, T.; Poulsen, H. F.; Schmidt, O.; Schneider, J. R.; Wolf, T.; Dosanjh, P.; Liang, R.; Hardy, W. N. Superstructure Formation and the Structural Phase Diagram of  $\text{YBa}_2\text{Cu}_3\text{O}_{6+x}$ . *Phys. C* **1999**, 317–318, 259–269.
- (7) Cava, R. J.; Hewat, A. W.; Hewat, E. A.; Batlogg, B.; Marezio, M.; Rabe, K. M.; Krajewski, J. J.; Peck, W. F.; Rupp, L. W. Structural Anomalies, Oxygen Ordering and Superconductivity in Oxygen Deficient  $\text{Ba}_2\text{YCu}_3\text{O}_x$ . *Phys. C* **1990**, 165, 419–433.
- (8) Eatough, M. O.; Ginley, D. S.; Morosin, B.; Venturini, E. L. Orthorhombic-tetragonal Phase Transition in High-temperature Superconductor  $\text{YBa}_2\text{Cu}_3\text{O}_7$ . *Appl. Phys. Lett.* **1987**, 51, 367–368.
- (9) Palau, A.; Fernandez-Rodriguez, A.; Gonzalez-Rosillo, J. C.; Granados, X.; Coll, M.; Bozzo, B.; Ortega-Hernandez, R.; Suñé, J.; Mestres, N.; Obradors, X.; Puig, T. Electrochemical Tuning of Metal Insulator Transition and Nonvolatile Resistive Switching in Superconducting Films. *ACS Appl. Mater. Interfaces* **2018**, 10, 30522–30531.
- (10) Marinković, S.; Fernández-Rodríguez, A.; Collienne, S.; Alvarez, S. B.; Melinte, S.; Maiorov, B.; Rius, G.; Granados, X.; Mestres, N.; Palau, A.; Silhanek, A. V. Direct Visualization of Current-Stimulated Oxygen Migration in  $\text{YBa}_2\text{Cu}_3\text{O}_{7-\delta}$  Thin Films. *ACS Nano* **2020**, 14, 11765–11774.
- (11) Murakami, M.; Sakai, N.; Higuchi, T.; Yoo, S. I. Melt-Processed Light Rare Earth Element - Ba - Cu - O. *Supercond. Sci. Technol.* **1996**, 9, 1015.
- (12) Yoshida, Y.; Ozaki, T.; Ichino, Y.; Takai, Y.; Matsumoto, K.; Ichinose, A.; Mukaida, M.; Horii, S. Progress in Development of Advanced PLD Process for High  $J_c$  REBCO Film. *Phys. C* **2008**, 468, 1606–1610.

- (13) Wee, S. H.; Goyal, A.; Martin, P. M.; Heatherly, L. High In-Field Critical Current Densities in Epitaxial  $\text{NdBa}_2\text{Cu}_3\text{O}_{7-\delta}$  Films on RABiTS by Pulsed Laser Deposition. *Supercond. Sci. Technol.* **2006**, *19*, 865–868.
- (14) Cayado, P.; Mundet, B.; Eloussifi, H.; Vallés, F.; Coll, M.; Ricart, S.; Gázquez, J.; Palau, A.; Roura, P.; Farjas, J.; Puig, T.; Obradors, X. Epitaxial Superconducting  $\text{GdBa}_2\text{Cu}_3\text{O}_{7-\delta}/\text{Gd}_2\text{O}_3$  Nanocomposite Thin Films from Advanced Low-Fluorine Solutions. *Supercond. Sci. Technol.* **2017**, *30*, 125010.
- (15) Cayado, P.; Erbe, M.; Kauffmann-Weiss, S.; Bühler, C.; Jung, A.; Hänisch, J.; Holzapfel, B. Large Critical Current Densities and Pinning Forces in CSD-Grown Superconducting  $\text{GdBa}_2\text{Cu}_3\text{O}_{7-x}$ - $\text{BaHfO}_3$  Nanocomposite Films. *Supercond. Sci. Technol.* **2017**, *30*, 094007.
- (16) Andreouli, C.; Tsetsekou, A. Synthesis of HTSC  $\text{Re}(\text{Y})\text{-Ba}_2\text{Cu}_3\text{O}_x$  Powders: The Role of Ionic Radius. *Phys. C* **1997**, *291*, 274–286.
- (17) MacManus-Driscoll, J. L.; Alonso, J. A.; Wang, P. C.; Geballe, T. H.; Bravman, J. C. Studies of Structural Disorder in  $\text{ReBa}_2\text{Cu}_3\text{O}_{7-x}$  Thin Films (Re=rare Earth) as a Function of Rare-Earth Ionic Radius and Film Deposition Conditions. *Phys. C* **1994**, *232*, 288–308.
- (18) MacManus-Driscoll, J. L.; Foltyn, S. R.; Jia, Q. X.; Wang, H.; Serquis, A.; Maiorov, B.; Civale, L.; Lin, Y.; Hawley, M. E.; Maley, M. P.; Peterson, D. E. Systematic Enhancement of In-Field Critical Current Density with Rare-Earth Ion Size Variance in Superconducting Rare-Earth Barium Cuprate Films. *Appl. Phys. Lett.* **2004**, *84*, 5329–5331.
- (19) MacManus-Driscoll, J. L.; Foltyn, S. R.; Maiorov, B.; Jia, Q. X.; Wang, H.; Serquis, A.; Civale, L.; Lin, Y.; Hawley, M. E.; Maley, M. P.; Peterson, D. E. Rare Earth Ion Size Effects and Enhanced Critical Current Densities in  $\text{Y}_{2/3}\text{Sm}_{1/3}\text{Ba}_2\text{Cu}_3\text{O}_{7-x}$  Coated Conductors. *Appl. Phys. Lett.* **2005**, *86*, 032505.
- (20) Gupta, A.; Jagannathan, R.; Cooper, E. I.; Giess, E. A.; Landman, J. I.; Hussey, B. W. Superconducting Oxide Films with High Transition Temperature Prepared from Metal Trifluoroacetate Precursors. *Appl. Phys. Lett.* **1988**, *52*, 2077–2079.
- (21) Obradors, X.; Puig, T. Coated Conductors for Power Applications: Materials Challenges. *Supercond. Sci. Technol.* **2014**, *27*, 044003.
- (22) Obradors, X.; Puig, T.; Pomar, A.; Sandiumenge, F.; Mestres, N.; Coll, M.; Cavallaro, A.; Romà, N.; Gázquez, J.; González, J. C.; Castaño, O.; Gutierrez, J.; Palau, A.; Zalamova, K.; Morlens, S.; Hassini, A.; Gibert, M.; Ricart, S.; Moretó, J. M.; Piñol, S.; Isfort, D.; Bock, J. Progress towards All-Chemical Superconducting  $\text{YBa}_2\text{Cu}_3\text{O}_7$ -Coated Conductors. *Supercond. Sci. Technol.* **2006**, *19*, S13.
- (23) Obradors, X.; Puig, T.; Pomar, A.; Sandiumenge, F.; Piñol, S.; Mestres, N.; Castaño, O.; Coll, M.; Cavallaro, A.; Palau, A.; Gázquez, J.; González, J. C.; Gutiérrez, J.; Romà, N.; Ricart, S.; Moretó, J. M.; Rossell, M. D.; Tendeloo, G. v. Chemical Solution Deposition: A Path towards Low Cost Coated Conductors. *Supercond. Sci. Technol.* **2004**, *17*, 1055.
- (24) Izumi, T.; Yoshizumi, M.; Matsuda, J.; Nakaoka, K.; Kitoh, Y.; Sutoh, Y.; Nakanishi, T.; Nakai, A.; Suzuki, K.; Yamada, Y.; Yajima, A.; Saitoh, T.; Shiohara, Y. Progress in Development of Advanced TFA-MOD Process for Coated Conductors. *Phys. C* **2007**, *463*–465, 510–514.
- (25) Grader, G. S.; Gallagher, P. K.; Thomson, J.; Gurvitch, M. Rates of Change in High Temperature Electrical Resistivity and Oxygen Diffusion Coefficient in  $\text{Ba}_2\text{YCu}_3\text{O}_x$ . *Appl. Phys. A* **1988**, *45*, 179–183.
- (26) Kittelberger, S.; Bolz, U.; Huebener, R. P.; Holzapfel, B.; Mex, L.; Schwarzer, R. A. Transient Local Resistivity Maximum during Temperature-Dependent Oxygen Diffusion in  $\text{YBa}_2\text{Cu}_3\text{O}_{7-\delta}$  Thin Films. *Phys. C* **1999**, *312*, 7–20.
- (27) Lee, S. H.; Bae, S. C.; Ku, J. K.; Shin, H. J. Oxygen Diffusion in Epitaxial  $\text{YBa}_2\text{Cu}_3\text{O}_{7-x}$  Thin Films. *Phys. Rev. B: Condens. Matter Mater. Phys.* **1992**, *46*, 9142–9146.
- (28) Kittelberger, S.; Bolz, U.; Huebener, R. P.; Holzapfel, B.; Mex, L. Oxygen Diffusion in  $\text{YBa}_2\text{Cu}_3\text{O}_{7-\delta}$  Films with Different Microstructures. *Phys. C* **1998**, *302*, 93–101.
- (29) Krauns, C.; Krebs, H.-U. Comparison of the Oxygen Diffusion in  $\text{YBa}_2\text{Cu}_3\text{O}_y$  Bulk Materials and Thin Films. *Z. Phys. B Condens. Matter* **1993**, *92*, 43–46.
- (30) Krebs, H.-U.; Krauns, C.; Mattheis, F. Oxygen Diffusion in Laser Deposited  $\text{YBaCuO}$  Thin Films. *J. Alloys Compd.* **1993**, *195*, 203–206.
- (31) Chen, L. L.; Chen, C. L.; Jacobson, A. J. Electrical Conductivity Relaxation Studies of Oxygen Transport in Epitaxial  $\text{YBa}_2\text{Cu}_3\text{O}_{7-y}$  Thin Films. *IEEE Trans. Appl. Supercond.* **2003**, *13*, 2882–2885.
- (32) Zhang, H.; Ye, H.; Du, K.; Huang, X. Y.; Wang, Z. H. Electric Resistance Relaxation and Oxygen Diffusion in Melt-Texture Grown YBCO Bulk Post-Annealed at High Temperature. *Supercond. Sci. Technol.* **2002**, *15*, 1268–1274.
- (33) Cayado, P.; Sánchez-Valdés, C. F.; Stangl, A.; Coll, M.; Roura, P.; Palau, A.; Puig, T.; Obradors, X. Untangling Surface Oxygen Exchange Effects in  $\text{YBa}_2\text{Cu}_3\text{O}_{6+x}$  Thin Films by Electrical Conductivity Relaxation. *Phys. Chem. Chem. Phys.* **2017**, *19*, 14129–14140.
- (34) Fick, A. Ueber Diffusion. *Ann. Phys.* **1855**, *170*, 59–86.
- (35) Crank, J. *The Mathematics of Diffusion*, 2nd ed.; Clarendon Press: Oxford, 1975.
- (36) Su, H.; Welch, D. O.; Wong-Ng, W. Strain Effects on Point Defects and Chain-Oxygen Order-Disorder Transition in 123 Cuprate Compounds. *Phys. Rev. B: Condens. Matter Mater. Phys.* **2004**, *70*, 054517.
- (37) Krekels, T.; Zou, H.; Van Tendeloo, G.; Wagener, D.; Buchgeister, M.; Hosseini, S. M.; Herzog, P. Ortho II Structure in  $\text{ABa}_2\text{Cu}_3\text{O}_{7-\delta}$  Compounds (A=Er, Nd, Pr, Sm, Yb). *Phys. C* **1992**, *196*, 363–368.
- (38) Macmanus-Driscoll, J. L. Materials Chemistry and Thermodynamics of  $\text{REBa}_2\text{Cu}_3\text{O}_{7-x}$ . *Adv. Mater.* **1997**, *9*, 457–473.
- (39) Liang, R.; Bonn, D. A.; Hardy, W. N. Evaluation of  $\text{CuO}$  2 Plane Hole Doping in  $\text{YBa}_2\text{Cu}_3\text{O}_{6+x}$  Single Crystals. *Phys. Rev. B: Condens. Matter Mater. Phys.* **2006**, *73*, 180505.
- (40) Cannelli, G.; Cantelli, R.; Cordero, F.; Trequattrini, F.; Ferraro, S.; Ferretti, M. Reordering Stages of Oxygen around 500 K in  $\text{REBa}_2\text{Cu}_3\text{O}_{6+x}$  by Anelastic Relaxation Measurements. *Solid State Commun.* **1991**, *80*, 715–718.
- (41) Rodríguez, E.; Gou, A.; Martínez, B.; Piñol, S.; Obradors, X. Influence of Disorder on the Vortex-Lattice Melting in Twinned Oxygen-Deficient Ortho-II  $\text{YBa}_2\text{Cu}_3\text{O}_y$  ( $y \approx 6.6$ ). *Phys. Rev. B: Condens. Matter Mater. Phys.* **1998**, *57*, 8687–8695.
- (42) Zhang, H.; Zou, X. W.; Wang, Z. H.; Chen, Y. X. A Comparative Investigation of Oxygen In-Diffusion in the Orthorhombic Phase of REBCO (RE: Y, Sm, Nd) by in Situ Electrical Resistance. *Phys. C* **2000**, *337*, 307.
- (43) Stangl, A.; Palau, A.; Deutscher, G.; Obradors, X.; Puig, T. Ultra-High Critical Current Densities of Superconducting  $\text{YBa}_2\text{Cu}_3\text{O}_{7-\delta}$  Thin Films in the Overdoped State. *Sci. Rep.* **2021**, *11*, 8176.
- (44) Talantsev, E. F.; Wimbush, S. C.; Strickland, N. M.; Xia, J. A.; D'Souza, P.; Storey, J. G.; Tallon, J. L.; Ingham, B.; Knibbe, R.; Long, N. J. Oxygen Deficiency, Stacking Faults and Calcium Substitution in MOD YBCO Coated Conductors. *IEEE Trans. Appl. Supercond.* **2013**, *23*, 7200205.
- (45) Shimoyama, J.-i.; Horii, S.; Otszchi, K.; Kishio, K. How to Optimize Critical Current Performance of RE123 Materials by Controlling Oxygen Content; *MRS Online Proceedings Library Archive 2001/ed*; Cambridge University Press, 2001; p 689.
- (46) Erbe, M.; Hänisch, J.; Freudenberg, T.; Kirchner, A.; Mönch, I.; Kaskel, S.; Schultz, L.; Holzapfel, B. Improved  $\text{REBa}_2\text{Cu}_3\text{O}_{7-x}$  (RE = Y, Gd) Structure and Superconducting Properties by Addition of Acetylacetone in TFA-MOD Precursor Solutions. *J. Mater. Chem. A* **2014**, *2*, 4932–4944.
- (47) Qu, T.; Xue, Y.; Feng, F.; Huang, R.; Wu, W.; Shi, K.; Han, Z. Study on the Oxygenation Process during the Heat Treatment of TFA-MOD YBCO Thin Films by in Situ Resistance Measurement. *Phys. C* **2013**, *494*, 148–152.

(48) Sánchez-Valdés, C. F.; Puig, T.; Obradors, X. In Situ study through Electrical Resistance of Growth Rate of Trifluoroacetate-Based Solution-Derived  $\text{YBa}_2\text{Cu}_3\text{O}_7$  Films. *Supercond. Sci. Technol.* **2015**, *28*, 024006.

(49) Chen, H.; Zalamova, K.; Pomar, A.; Granados, X.; Puig, T.; Obradors, X. Growth Rate Control and Solid–Gas Modeling of TFA- $\text{YBa}_2\text{Cu}_3\text{O}_7$  Thin Film Processing. *Supercond. Sci. Technol.* **2010**, *23*, 034005.

(50) Chen, H.; Zalamova, K.; Pomar, A.; Granados, X.; Puig, T.; Obradors, X. Nucleation and Growth Rate Influence on Microstructure and Critical Currents of TFA- $\text{YBa}_2\text{Cu}_3\text{O}_7$  under Low-Pressure Conditions. *J. Mater. Res.* **2010**, *25*, 2371–2379.

(51) Nelson, J. B.; Riley, D. P. The Thermal Expansion of Graphite from 15 c. to 800 c.: Part I. Experimental. *Proc. Phys. Soc.* **1945**, *57*, 477–486.

(52) Nelson, J. B.; Riley, D. P. An Experimental Investigation of Extrapolation Methods in the Derivation of Accurate Unit-Cell Dimensions of Crystals. *Proc. Phys. Soc.* **1945**, *57*, 160–177.